

## Supporting Information

# Exploring the effect of acid modulators on MIL-101 (Cr) metal-organic framework catalysed olefin-aldehyde condensation; A sustainable approach for the selective synthesis of nopol

Bhavana B. Kulkarni,<sup>a,b</sup> Kempanna S. Kanakikodi, <sup>a,b</sup>Dheer A. Rambhia, <sup>c</sup>Suresh Babu. Kalidindi, <sup>d</sup>Sanjeev P. Maradur<sup>a\*</sup>

<sup>a</sup> Materials & Catalysis Division, Poornaprajna Institute of Scientific Research (PPISR), Bidalur Post, Devanahalli, Bangalore-562164, Karnataka State, India.

<sup>b</sup> Graduate studies, Manipal Academy of Higher Education, Manipal -576104, Karnataka, India.

<sup>c</sup> Department of Chemistry, Institute of Chemical Technology (ICT), Mumbai, 400019, India.

<sup>d</sup> Inorganic and Analytical Chemistry Department, School of Chemistry, Andhra University, Visakhapatnam, India-530003.

### \*Corresponding author

Tel: +91(080)27408552

Fax: +91 23619034

E-mail: [sanjeevpm@poornaprajna.org](mailto:sanjeevpm@poornaprajna.org)

## **Figures**

**Figure S1.**Pyridine FTIR spectra of MIL-101(Cr) catalysts

**Figure S2.** Plausible mechanism for the Prins condensation of  $\beta$ -pinene with p-formaldehyde over MIL-101(Cr) catalyst

**Figure S3.**PXRD profile of spent MIL-101(AA) catalyst

**Figure S4.** $N_2$  sorption isotherm of spent MIL-101(AA) catalyst

**Figure S5.**TGA profile of spent MIL-101(AA) catalyst

**Figure S6.**FTIR spectra of spent MIL-101(AA) catalyst

**Figure S7.** Py-FTIR spectra of spent MIL-101(AA) catalyst

## **Tables**

**Table S1.** Selected literature on the Prins Condensation of  $\beta$ -pinene with p-formaldehyde

**Table S2.**Solvent properties

**Table S3.** Textural and surface acidic properties of spent MIL-101(AA) catalyst obtained from  $N_2$  sorption at 77K and  $NH_3$ -TPD analysis

**Table S4.** Comparison of various kinetic models

**Figure S1.**Pyridine FTIR spectra of MIL-101(Cr) catalysts

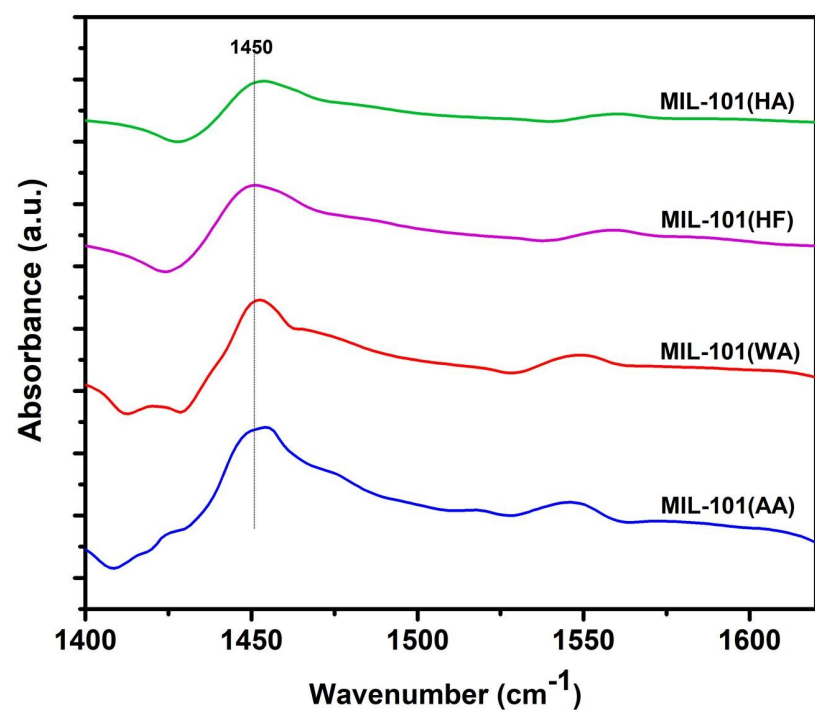


**Figure S2.** Plausible mechanism for the Prins condensation of  $\beta$ -pinene with p-formaldehyde

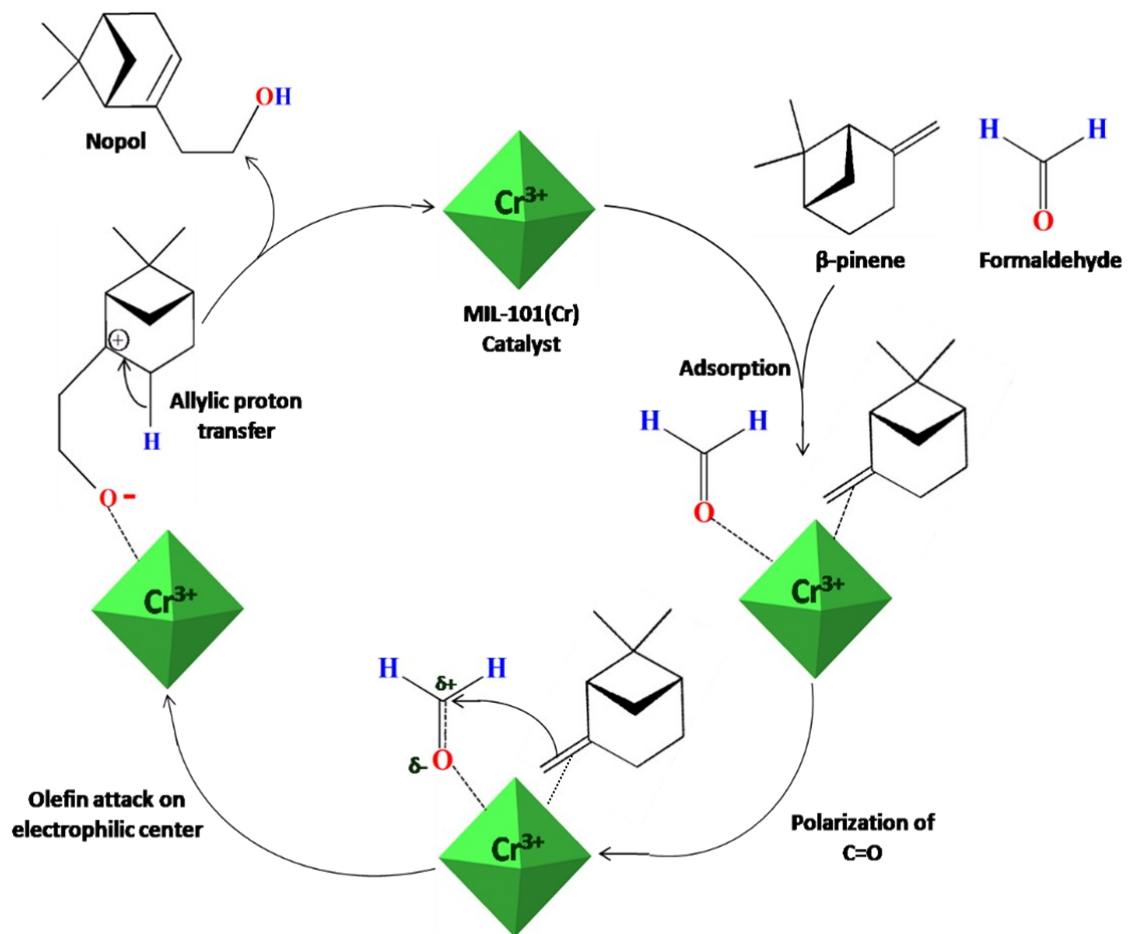


**Figure S3. PXRD profile of spent MIL-101(AA) catalyst**

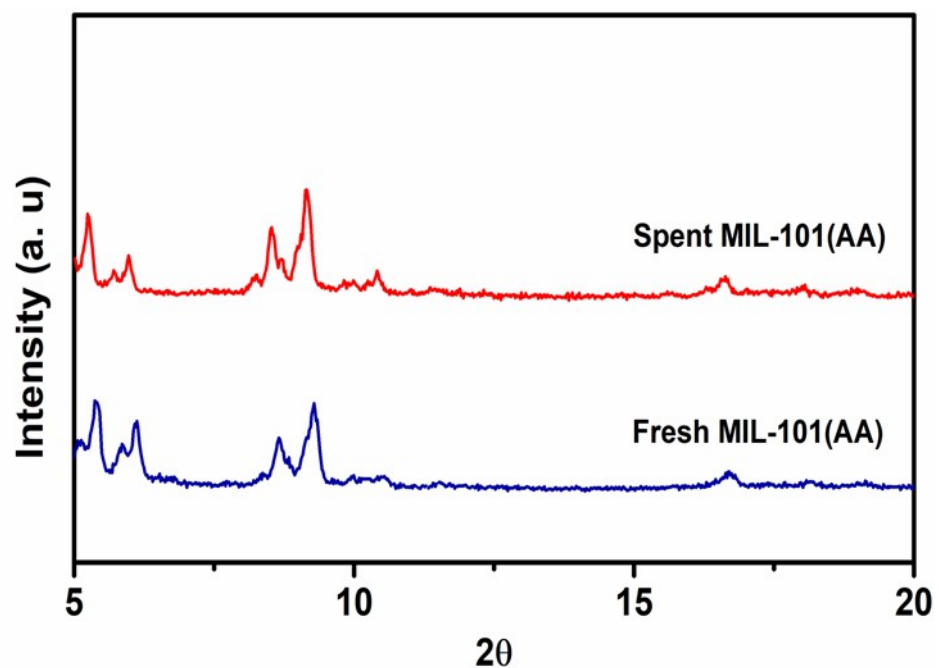


**Figure S4. N<sub>2</sub> sorption isotherm of spent MIL-101(AA) catalyst**

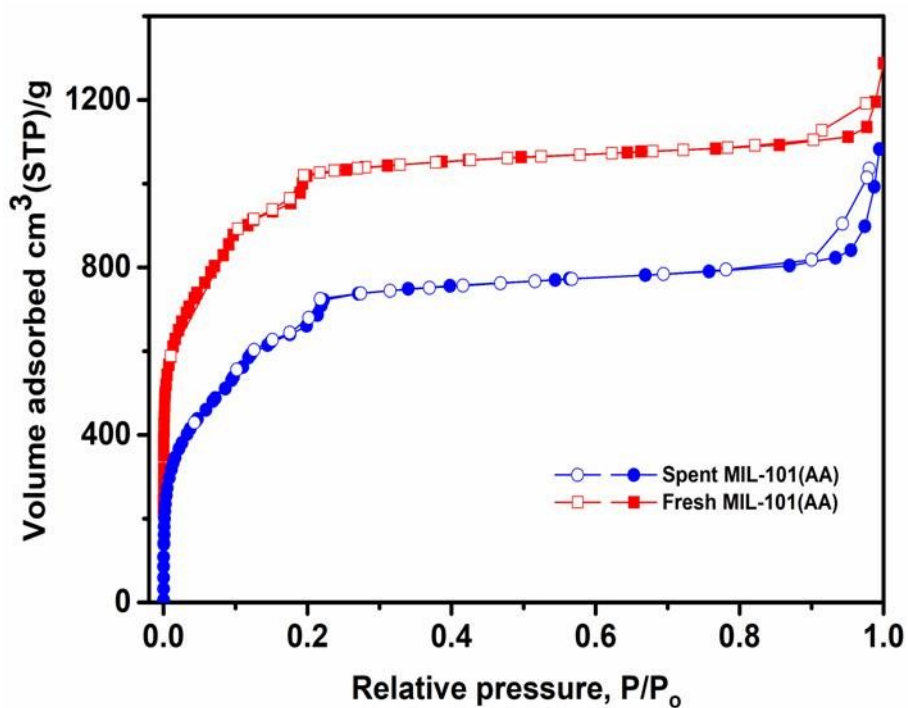


**Figure S5.** TGA profile of spent MIL-101(AA) catalyst

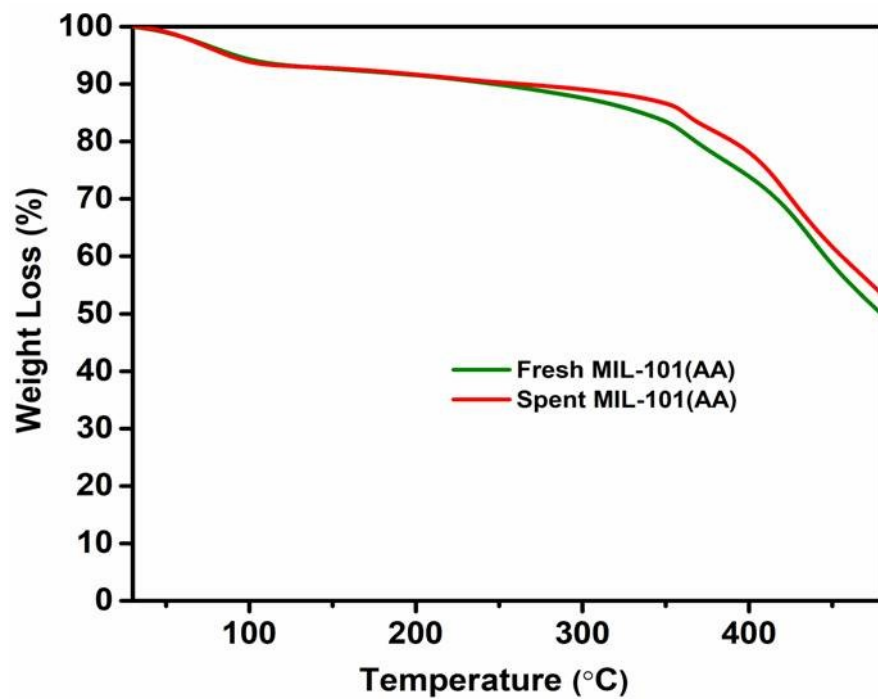


**Figure S6.** FTIR spectra of spent MIL-101(AA) catalyst

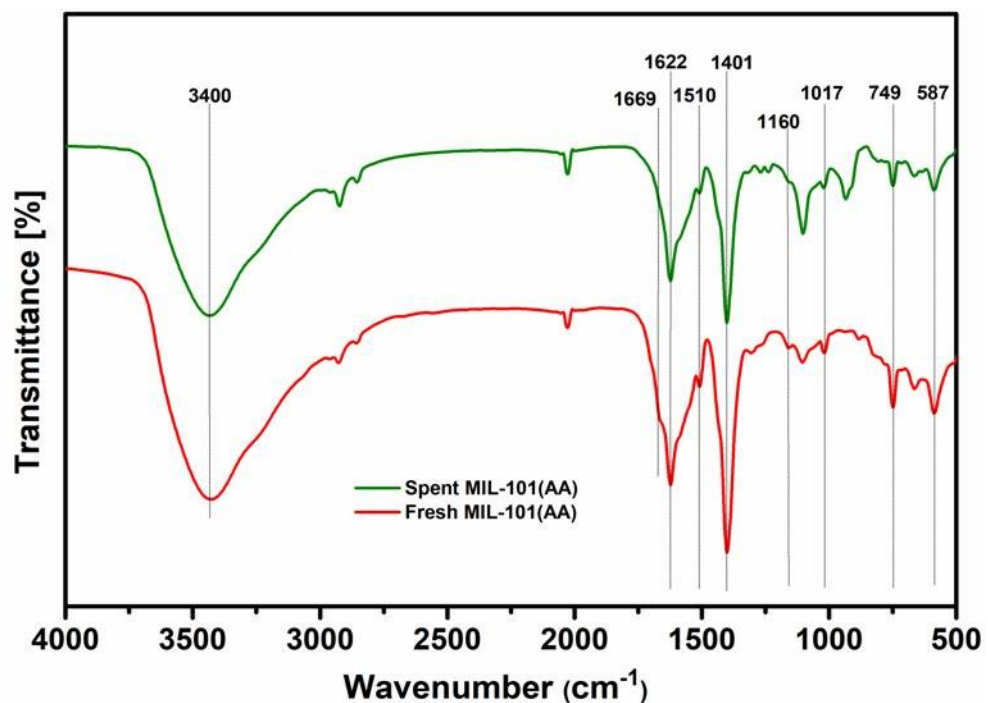


**Figure S7. Py-FTIR spectra of spent MIL-101(AA) catalyst**

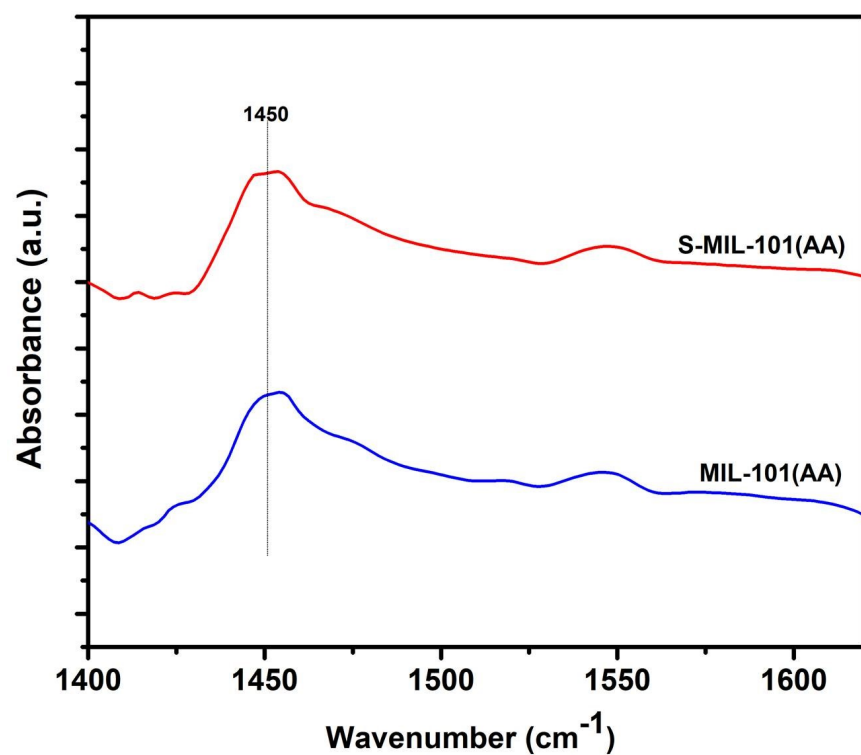


**Table S1.** Selected literature on the Prins Condensation of  $\beta$ -pinene with p-formaldehyde

Sl. no.	Catalyst	Cat. (Wt.%)	<sup>a</sup> Mole ratio	Time (h)	Temp. (°C)	Solvent	Conv. (%)	<sup>b</sup> Sel. (%)	TOF	Ref.
1	MIL-100(Fe)	25.5	2.0	5.0	80.0	Acetonitrile	82	-	2.2	[1]
2	MIL-100(Fe,Ni)	9.0	1.0	10.0	80.0	Acetonitrile	90	-	NA	[2]
3	Fe-BTC	25.5	2.0	6.0	80.0	Acetonitrile	47	100	0.7	[3]
4	0.94Zr-MCM-41(550)	25.5	2.0	6.0	90.0	Toluene	97	90	23.1	[4]
5	Zn-Al-MCM-41(151)	143.2	1.7	6.0	90.0	Toluene	75	94	4.9	[5]
6	FePO4	50.9	2.0	6.0	80.0	Acetonitrile	82	100	NA	[6]
7	Fe-Zn-DMC	10.2	2.0	12.0	80.0	Toluene	90	-	1.9	[7]
8	Sn-MCM-41	144.2	2.0	6.5	90.0	Toluene	98	80	NA	[8]
9	Zn-Beta	20.0	2.0	10.0	90.0	Benzonitrile	92	85	1.2	[9]
10	SZF-470	12.4	3.0	12.0	95.0	Toluene	70	88	3.8	[10]
11	SnMB16	50.9	2.0	1.0	90.0	Toluene	95	79	237. 1	[11]
12	Sn-MCM-41-D1	50.9	2.0	1.0	90.0	Toluene	99	98	NA	[12]
13	Sn-SBA-15	12.7	2.0	6.0	90.0	Toluene	99	95	NA	[13]
14	SZ-2N	11.0	3.0	9.0	80.0	Acetonitrile	99	99	3.7	[14]
15	SnO2-T-350	383.7	0.4	10.0	90.0	Benzonitrile	80	93	0.2	[15]
16	Na-ZrO2-ZrP-a-350	25.5	2.0	4.0	80.0	Toluene	86	87	11.9	[16]
17	10Zr-208-8	25.5	2.0	6.0	80.0	Toluene	74	100	4.8	[17]
18	MoOx/ $\gamma$ -Al2O3	20.0	2.0	10.0	90.0	Benzonitrile	96	86	2.7	[18]
19	SnCl2-I-24	24.5	2.0	3.0	90.0	Toluene	79	86	NA	[19]
20	Zn-MMT	10.2	2.0	24.0	80.0	Acetonitrile	75	97	NA	[20]
21	<b>MIL-101(AA)</b>	<b>5.0</b>	<b>2.0</b>	<b>6.0</b>	<b>90.0</b>	<b>Benzonitrile</b>	<b>98</b>	<b>&gt;99</b>	<b>18.9</b>	<b>CW</b>
22	<b>MIL-101(WA)</b>	<b>5.0</b>	<b>2.0</b>	<b>6.0</b>	<b>90.0</b>	<b>Benzonitrile</b>	<b>86</b>	<b>&gt;99</b>	<b>23.2</b>	<b>CW</b>
23	<b>MIL-101(HF)</b>	<b>5.0</b>	<b>2.0</b>	<b>6.0</b>	<b>90.0</b>	<b>Benzonitrile</b>	<b>80</b>	<b>&gt;99</b>	<b>24.7</b>	<b>CW</b>
24	<b>MIL-101(HA)</b>	<b>5.0</b>	<b>2.0</b>	<b>6.0</b>	<b>90.0</b>	<b>Benzonitrile</b>	<b>58</b>	<b>&gt;99</b>	<b>25.2</b>	<b>CW</b>
25	<b>MIL-101(AA)</b>	<b>5.0</b>	<b>2.0</b>	<b>3.0</b>	<b>90.0</b>	<b>Benzonitrile</b>	<b>67</b>	<b>&gt;99</b>	<b>25.9</b>	<b>CW</b>

<sup>a</sup>- Mole ratio ( $\beta$ -pinene top-formaldehyde)<sup>b</sup>- Nopol selectivity

TOF- Turn-over frequency

NA- Not available

CW- Current work

**Table S2.**Solvent properties

Solvent	AN	DN	BP (°C)	DC	HSP (MPa) <sup>1/2</sup>
Acetonitrile	18.9	14.1	82	37.5	24.3
Benzonitrile	15.5	11.9	191	26.0	19.9
Nitrobenzene	14.8	4.4	210.9	34.8	22.2
Toluene	8.2	0	110.6	2.4	18.2
Cyclohexane	0	0	80.75	2.0	16.7

**AN:** Acceptor number

**DN:** Donor number

**BP:** Boiling point

**DC:** Dielectric constant

**HSP:** Hansen's solubility parameter

**Table S3. Textural and surface acidic Properties of spent MIL-101(AA) catalyst obtained from N<sub>2</sub> sorption at 77K and NH<sub>3</sub>-TPD analysis**

Sample	S <sub>BET</sub> <sup>a</sup> (m <sup>2</sup> g <sup>-1</sup> )	V <sub>total</sub> <sup>b</sup> (cm <sup>3</sup> g <sup>-1</sup> )	D <sub>p</sub> <sup>c</sup> (nm)	Acidity <sup>d</sup> (mmol g <sup>-1</sup> )
Fresh MIL-101(AA)	3014	1.75	2.32	0.88
Spent-MIL-101(AA)	2867	1.62	2.34	0.78

<sup>a</sup>S<sub>BET</sub> is the specific surface area determined by Brunauer-Emmett-Teller (BET) method

<sup>b</sup>V<sub>total</sub> is the total pore volume at  $p/p_0 = 0.990$

<sup>c</sup>D<sub>p</sub> is the mean pore diameter

<sup>d</sup>Acidity of the material calculated from NH<sub>3</sub>-TPD measurement

**Table S4. Comparison of various kinetic models**

No.	Kinetic Model	$R^2$	Linearized kinetic parameter equations	$R_i^2$
M1	$R = \frac{K_s(C_F C_B)}{\{1 + K_F C_F\}}$	0.989	$\ln K_F = \frac{9225.1}{T} - 23.37$ $\ln K_n = \frac{-12317}{T} + 35.747$ $\ln K_S = \frac{7167}{T} - 16.53$	$R_{kf}^2 = 0.967$ $R_{kn}^2 = 0.9547$
M2	$R = \frac{K_s(C_F C_B)}{\{1 + K_F C_F + K_N C_N\}}$	0.988	$\ln K_F = \frac{3759}{T} - 101.33$ $\ln K_n = \frac{-9693}{T} + 28.96$ $\ln K_S = \frac{13204}{T} - 33.59$	$R_{kf}^2 = 0.807$ $R_{kn}^2 = 0.7951$ $R_{ks}^2 = 0.9772$
M3	$R = \frac{K_s(C_F C_B - C_N/K_c)}{\{1 + K_F C_F + K_N C_N\}}$	0.988	$\ln K_F = \frac{39980}{T} - 108.33$ $\ln K_n = \frac{-8644}{T} + 25.99$ $\ln K_S = \frac{9225.1}{T} - 23.37$	$R_{kf}^2 = 0.9992$ $R_{kn}^2 = 0.8229$ $R_{ks}^2 = 0.8892$
M4	$R = \frac{K_s(C_F C_B)}{\{1 + K_F C_F\}^2}$	0.959	$\ln K_F = \frac{-12317}{T} + 35.747$ $\ln K_S = \frac{9434.7}{T} - 23.91$	$R_{kf}^2 = 0.967$ $R_{ks}^2 = 0.9547$
M5	$R = \frac{K_s(C_F C_B)}{\{1 + K_F C_F + K_B C_B + K_N C_N\}^2}$	0.989	$\ln K_B = \frac{14564}{T} - 37.792$ $\ln K_n = \frac{12928}{T} - 33.257$ $\ln K_S = \frac{-12317}{T} + 35.74$	$R_{kB}^2 = 0.9978$ $R_{kn}^2 = 0.9314$ $R_{ks}^2 = 0.998$
M6	$R = \frac{K_s(C_F C_B - C_N/K_c)}{\{1 + K_F C_F + K_B C_B + K_N C_N\}^2}$	0.991	$\ln K_F = \frac{8495}{T} - 20.73$ $\ln K_B = \frac{39571}{T} - 106.9$ $\ln K_n = \frac{2558}{T} - 4.332$ $\ln K_S = \frac{-7367.9}{T} + 22.858$	$R_{kf}^2 = 0.991$ $R_{kB}^2 = 0.775$ $R_{kn}^2 = 0.7033$ $R_{ks}^2 = 0.8892$

$R^2$ : Coefficient of determination between the experimental and simulated model

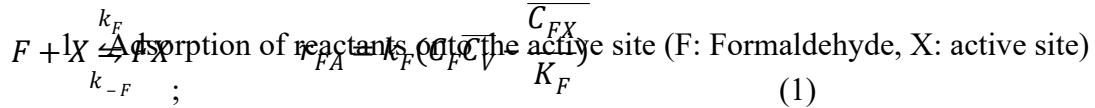
$K_{F,B,N}$ : Adsorption constants of formaldehyde,  $\beta$ -Pinene and nopol

$K_s$ : Reaction constant

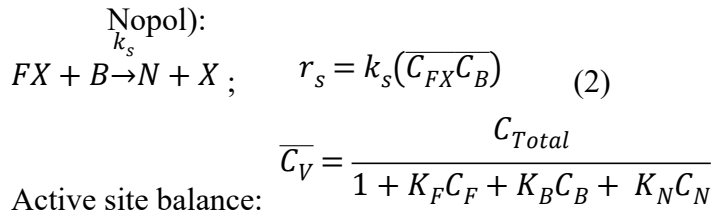
$R_i^2$  : Coefficient of determination of linear fitting of kinetic parameters; i represents the corresponding subscript used in kinetic constants  $K_i$ .

Models M1, M2 and M3 are based on a single site mechanism with the adsorption of formaldehyde onto the active site and its reaction with  $\beta$ -pinene present in the liquid phase. M1 considers the formation of nopol without its adsorption onto the active site, while M2 considers nopol adsorption, and M3 considers nopol adsorption with a possible reversible reaction. Models M4, M5 and M6 are based on a dual site mechanism with the adsorption of formaldehyde and  $\beta$ -pinene onto the active site and their reaction to yield nopol, which later desorbs into the liquid phase. M4 considers the relatively strong adsorption of formaldehyde while M5 considers an irreversible reaction and M6 considers the reversible reaction

M1 Model derivation:



2. Surface reaction on the dual sites and the formation of product (B:  $\beta$ -Pinene, N:



$$R = \frac{K(C_F C_B)}{\frac{dX}{dt} + K_F C_F} \quad (K = C_{Total} \times K_F \times K_B) \quad (M1)$$

$$R = \frac{dX}{dt} W_{cat} \quad \text{eqn. 1}$$

Mole balance of  $\beta$ -Pinene throughout the reaction is calculated by eqn. 1 and this ode was solved using ode45 solver in MATLAB while the unknown adsorption and reaction constants were estimated using genetic algorithm as an optimization function. The objective function f used to calculate the coefficient of determination eqn 2. was optimized using GA to yield a minimum error. Default parameters of genetic algorithm optimization were used with a population size of 200.

$$f = \sum_{i=0}^n (C_{B,Exp}^i - C_{B,Thr}^i)^2 \quad \text{eqn. 2}$$

## References

- [1] M. Opanasenko, A. Dhakshinamoorthy, Y.K. Hwang, J.S. Chang, H. Garcia, J. Čejka, Superior performance of metal–organic frameworks over zeolites as solid acid catalysts in the Prins reaction: green synthesis of nopol, *ChemSusChem*, 6 (2013) 865-871.
- [2] M. Giménez-Marqués, A. Santiago-Portillo, S. Navalón, M. Álvaro, V. Briois, F. Nouar, H. Garcia, C. Serre, Exploring the catalytic performance of a series of bimetallic MIL-100 (Fe, Ni) MOFs, *Journal of Materials Chemistry A*, 7 (2019) 20285-20292.
- [3] M. Shamzhy, M. Opanasenko, O. Shvets, J. Čejka, Catalytic performance of Metal-Organic-Frameworks vs. extra-large pore zeolite UTL in condensation reactions, *Frontiers in chemistry*, 1 (2013) 11.
- [4] X. Chu, D. Zhou, D. Li, K. Xia, N. Gan, X. Lu, R. Nie, Q. Xia, Construction of solely Lewis acidic sites on Zr-MCM-41 and the catalytic activity for the Prins condensation of  $\beta$ -pinene and paraformaldehyde to nopol, *Microporous and Mesoporous Materials*, 230 (2016) 166-176.
- [5] M. Selvaraj, S. Kawi, Highly selective synthesis of nopol over mesoporous and microporous solid acid catalysts, *Journal of Molecular Catalysis A: Chemical*, 246 (2006) 218-222.
- [6] U.R. Pillai, E. Sahle-Demessie, Mesoporous iron phosphate as an active, selective and recyclable catalyst for the synthesis of nopol by Prins condensation, *Chemical communications*, (2004) 826-827.
- [7] M.V. Patil, M.K. Yadav, R.V. Jasra, Prins condensation for synthesis of nopol from  $\beta$ -pinene and paraformaldehyde on novel Fe–Zn double metal cyanide solid acid catalyst, *Journal of Molecular Catalysis A: Chemical*, 273 (2007) 39-47.
- [8] A.L. Villa Holguín, E.A. Alarcón Durango, C. Montes de Correa, Synthesis of nopol over MCM-41 catalysts, (2002).
- [9] V.S. Marakatti, A.B. Halgeri, G.V. Shanbhag, Metal ion-exchanged zeolites as solid acid catalysts for the green synthesis of nopol from Prins reaction, *Catalysis Science & Technology*, 4 (2014) 4065-4074.
- [10] S.V. Jadhav, K.M. Jinka, H.C. Bajaj, Nanosized sulfated zinc ferrite as catalyst for the synthesis of nopol and other fine chemicals, *Catalysis today*, 198 (2012) 98-105.
- [11] E.A. Alarcón Durango, A.L. Villa Holguín, C. Montes de Correa, Characterization of Sn-and Zn-loaded MCM-41 catalysts for nopol synthesis, (2009).
- [12] A. de P, E. Alarcón, C. de C, Nopol synthesis over Sn-MCM-41 and Sn-kenyaite catalysts, *Catalysis Today*, 107 (2005) 942-948.
- [13] M. Selvaraj, Y. Choe, Well ordered two-dimensional SnSBA-15 catalysts synthesized with high levels of tetrahedral tin for highly efficient and clean synthesis of nopol, *Applied Catalysis A: General*, 373 (2010) 186-191.
- [14] S.V. Jadhav, K.M. Jinka, H.C. Bajaj, Synthesis of nopol via Prins condensation of  $\beta$ -pinene and paraformaldehyde catalyzed by sulfated zirconia, *Applied Catalysis A: General*, 390 (2010) 158-165.
- [15] P. Manjunathan, G.V. Shanbhag, Application of tin oxide-based materials in catalysis, in: *Tin Oxide Materials*, Elsevier, 2020, pp. 519-553.
- [16] X. Wang, T. Wang, W. Hua, Y. Yue, Z. Gao, Synthesis of zirconia porous phosphate heterostructures (Zr-PPH) for Prins condensation, *Catalysis Communications*, 43 (2014) 97-101.
- [17] D.M. Do, S. Jaenicke, G.-K. Chuah, Mesoporous Zr-SBA-15 as a green solid acid catalyst for the Prins reaction, *Catalysis Science & Technology*, 2 (2012) 1417-1424.
- [18] V.S. Marakatti, D. Mumbaraddi, G.V. Shanbhag, A.B. Halgeri, S.P. Maradur, Molybdenum oxide/ $\gamma$ -alumina: an efficient solid acid catalyst for the synthesis of nopol by Prins reaction, *RSC advances*, 5 (2015) 93452-93462.
- [19] E.A. Alarcón, L. Correa, C. Montes, A.L. Villa, Nopol production over Sn-MCM-41 synthesized by different procedures–Solvent effects, *Microporous and mesoporous materials*, 136 (2010) 59-67.
- [20] M.K. Yadav, R.V. Jasra, Synthesis of nopol from  $\beta$ -pinene using ZnCl<sub>2</sub> impregnated Indian Montmorillonite, *Catalysis Communications*, 7 (2006) 889-895.